Eur. Phys. J. B **9**, 471–477 (1999)

THE EUROPEAN PHYSICAL JOURNAL B

EDP Sciences

Dynamics of reorientation of a constrained nematic elastomer

P.I.C. Teixeira[a]

Cavendish Laboratory, University of Cambridge, Madingley Road, Cambridge CB3 0HE, UK

Received 22 June 1998

Abstract. A model is proposed for the reorientation dynamics of a confined nematic liquid crystal elastomer, where the effect of crosslinks is to couple the director to deformations of the elastic matrix. The model combines the (equilibrium) 'neo-classical' theory of liquid crystal rubber elasticity with the simplest time evolution equations for a system described by two coupled, non-conserved order parameters. Relaxation from an orientation imposed by an electric field is studied as a function of elastic softness, starting angle, surface pretilt, and the relative mobilities of director and strain. Most importantly, the absence of a 'semi-soft' elastic threshold changes the long-time behaviour of the effective refractive index of the medium from exponential to inverse power law decay. Predictions are compatible with recent experimental results by Chang, Chien and Meyer [Phys. Rev. E **56**, 595 (1997)].

PACS. 61.30.Cz Theory and models of liquid crystal structure – 61.41.+e Polymers, elastomers, and plastics

1 Introduction

Liquid crystalline elastomers, also known as solid liquid crystals, consist of (typically weakly) crosslinked polymer liquid crystals, and combine the extensional properties of rubber with the easy orientability of the conventional mesophases. For this reason they may be termed anisotropic rubbers. Their existence was postulated by de Gennes [1,2]; they were subsequently synthesised by Finkelmann's and Mitchell's groups, as well as by a number of others (see, *e.g.*, [3] and references therein). Theoretical progress in this area has been reviewed by Warner and Terentjev [4].

Because mesogenic polymer chains will stretch or flatten on ordering orientationally, the coupling between director and polymer matrix in elastomers leads to macroscopic sample shape changes [5,6]. This is but one of the many exotic properties exhibited by these materials; others include memory effects [7] and stress-induced molecular switching [8]. In addition, Bladon, Terentjev and Warner [9,10] predicted that application of a strain perpendicular to the direction of liquid crystal (LC) alignment (the director) could induce discontinuous director rotation. This is sometimes referred to as an 'anti-Frederiks' transition, as the nematic is anchored in bulk (to the polymer matrix) and rotates under the influence of a mechanical field imposed at the surfaces. Such a transition was indeed observed experimentally by Mitchell and co-workers [11,12], while Kundler and Finkelmann [13] have reported a more intriguing variant of the same phenomenon, where evolution between the initial and final states, characterised respectively by the director lying perpendicular or parallel to the direction of applied strain, proceeds *via* an intermediate, non-uniform 'stripe-domain' state. Terentjev and Warner [14,15] have interpreted the latter result in terms of their molecular theory of elastomers [16], which is able to deal with non-linearities and discontinuities.

In another recent development, Meyer and co-workers reported an electro-optical study of a confined nematic elastomer gel [17]. Switching of this material by an applied electrical field differs in several important respects from the Frederiks transition in ordinary nematics. Firstly, it is characterised by a threshold *field*, rather than voltage. Secondly, this field is much higher than expected for an ordinary Frederiks cell, which indicates that the relevant length scale in the system is much smaller than the film thickness. Finally, uniaxial symmetry is preserved at all stages of switching. These results have been explained by assuming that, as a consequence of network formation in the nematic phase, an anisotropic gel is uniformly distributed throughout the LC which produces a mean orienting effect described as an effective internal field applied along the director. The external field would then 'see' the lengthscale of static director distortions perpendicular to this effective internal field, rather than the whole film thickness.

Although the above picture fits the experimental data reasonably well, a new length scale has to be invoked in order to give an interpretation in terms of a classical

[a] *Present address*: IRC in Polymer Science and Technology, Department of Physics and Astronomy, University of Leeds, Leeds LS2 9JT, United Kingdom.
e-mail: phypt@irc.leeds.ac.uk

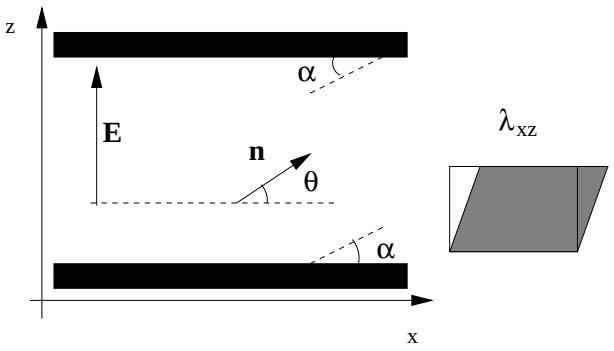

Fig. 1. Experimental geometry considered: At $t = 0$, the nematic director $\mathbf{n}$ makes an angle θ_0 with the x-axis. On switching off the field $\mathbf{n}$, parametrised by the angle θ, relaxes towards the pretilt α induced by the bounding plates. The only allowed strain is λ_{xz}, which relaxes to zero.

Frederiks transition. It would be more natural to look to the theory of nematic elastomers for a description. The first, linear, continuum picture of these materials is due to de Gennes [18], who wrote down a (phenomenological) free energy density in terms of two energy scales D_1 and D_2. These penalise, respectively, director rotations with respect to the polymer matrix, and shear deformations of the polymer matrix relative to the director. However, the only way fully to account for non-linearities and discontinuities, is to use a molecular approach. Terentjev and co-workers [19] have shown that the neo-classical theory of elastomers [4] predicts the existence of a threshold field as a consequence of the fact that, in a nematic elastomer, the director is anchored in *bulk* to the elastic network. The same theory also explains why the symmetry of the observed pattern remains uniaxial during the experiment.

Here I employ the above microscopic formalism to model relaxation from an externally-imposed orientation. This is inspired by the dynamical results reported in [17], but not restricted to their interpretation; rather, it is attempted to extract the general trends of such non-equilibrium behaviour as functions of elastomer material parameters, initial orientation and boundary conditions. This paper is organised as follows: in Section 2 the static theory of [19], upon which the present work is based, is briefly summarised. The dynamical model is then introduced, and its evolution equations solved in Section 3. Finally in Section 4 the relevance of the present theory to Meyer's findings is discussed.

2 Theory

2.1 The free energy

Consider, as in [19], a macroscopically uniform sample of nematic elastomer sandwiched between two aligning plates inducing a (typically small) pretilt α (see Fig. 1). This is the standard 'splay' geometry for the Frederiks transition. We assume that, when an electric field is applied perpendicular to the plane of the cell, the director $\mathbf{n}$ rotates in the xz-plane and is parametrised by the angle θ it makes with the x-axis, which is a function of the coordinate z only (see Fig. 1). It is also useful to define the angle by which reorientation occurs, $\omega = \theta - \alpha$. As discussed in [19], in an elastomer any director rotation is associated with an elastic deformation. In particular, a rotation in the xz-plane may give rise to non-zero strain tensor components λ_{xx}, λ_{zz} (and λ_{yy} *via* the incompressibility constraint), as well as, foremostly, to the shears λ_{xz} and λ_{zx} – all of which can be functions of z. Restrictions arise, however, from the requirement of mechanical (in fact geometrical) compatibility, $\partial\lambda_{ij}/\partial x_i = \partial\lambda_{ii}/\partial x_j$. Whence if, *e.g.*, $\lambda_{xx}(z) \neq 1$, then λ_{xz} must be a function of x, contrary to our assumption of pure z-dependence; likewise, $\lambda_{zx}(z) \neq 0$ implies $\lambda_{zz}(x)$, *etc.* The only simple way out seems to be to have just a shear $\lambda_{xz}(z)$ while keeping all other components of the strain tensor constant:

$$\lambda = \begin{pmatrix} 1 & 0 & \lambda_{xz} \\ 0 & 1 & 0 \\ 0 & 0 & 1 \end{pmatrix}, \tag{1}$$

and consequently we are left with just two relevant variables, θ and λ_{xz}. In this paper we restrict ourselves to spatially homogeneous strains and tilts (see below), but retain the above form with a view to future generalisations of the formalism.

The neo-classical free energy density (FED) of a semi-soft nematic rubber is then [4,19],

$$f = \frac{1}{2}\mu \mathsf{Tr}\left[\ell_0 \lambda^T \ell^{-1} \lambda\right] + \frac{1}{2}\mu A \left[\sin(\theta - \alpha) - \lambda_{xz}\cos\theta\cos\alpha\right]^2 - \frac{1}{2}\varepsilon_0 \Delta\varepsilon E^2 \sin^2\theta, \tag{2}$$

where $\mu = n_\times k_\mathrm{B} T$ is the rubber energy scale (with $n_\times$ the number of chain strands per unit volume), ℓ is the persistence length tensor describing the chain shape (the subscript 0 referring to the state prior to the deformation), A is the semi-soft parameter, E the applied electric field, ε_0 the dielectric permitivity of the vacuum, and $\Delta\varepsilon$ the dielectric anisotropy of the LC elastomer. In its principal axes frame, ℓ can be written as:

$$\ell = \begin{pmatrix} \ell_\parallel & 0 & 0 \\ 0 & \ell_\perp & 0 \\ 0 & 0 & \ell_\perp \end{pmatrix} = \ell_\perp \begin{pmatrix} r & 0 & 0 \\ 0 & 1 & 0 \\ 0 & 0 & 1 \end{pmatrix}, \tag{3}$$

where $r = \ell_\parallel/\ell_\perp$ is the ratio of principal chain step lengths (chain anisotropy). If the director $\mathbf{n}$ is rotated by Ω in the xz-plane, then $\ell(\Omega) = R^T(\Omega)\ell R(\Omega)$, $R(\Omega)$ being the appropriate (in this case two-dimensional) rotation matrix [20]. Finally, the semi-soft elasticity coefficient A subsumes all the (microscopic) sources of inhomogeneity (fluctuations in the composition, or the length, of strands between crosslinks, impurities, ...) that act as barriers to rotation; these are discussed in more detail elsewhere [15]. When $A = 0$ (soft elasticity) there exist deformations of the unconstrained elastomer which cost no energy, therefore the threshold strain for such deformations in a given material will give a measure of A; typically, $A \ll 1$.

Equation (2) is a generalisation of equation (3) of [19] to the case of nonzero pretilt. The static analysis of [19] now proceeds by minimising the FED with respect to λ_{xz} and θ (in this order), thereby obtaining an expression for the optimal director angle $\theta(E)$. The existence of a threshold *field* E_c is thus immediately revealed which is a function of the chain anisotropy r and of the semi-softness A.

In what follows we shall neglect inhomogeneities, *i.e.*, assume both strain and director to be spatially uniform, hence the absence of gradient terms in equation (2). This is to be expected from the fact that the rubber energy scale is much larger than that of LC elasticity [21]; and appears to be confirmed by direct observation [17]. In addition, in [19] the static features of the Frederiks transition have been successfully modelled, *for the two sample thicknesses investigated*, under the assumption of spatial homogeneity, which lends it strong support. Note, however, that in nematic solids *uniform* rotations are also penalised.

Only the dynamics of relaxation upon removal of the external field will be considered, so we set $E = 0$. Using equations (2, 3), the reduced FED becomes

$$\begin{aligned}\frac{2f}{\mu} = 3 + \frac{(r-1)^2}{r}\sin^2(\theta-\alpha) + \frac{r-1}{r}\lambda_{xz}\sin(\theta-\alpha) \\ \times\left[(r+1)\cos(\theta+\alpha) - (r-1)\cos(\theta-\alpha)\right] \\ + \frac{\lambda_{xz}^2}{r}\left[1+(r-1)\sin^2\alpha\right]\left[1+(r-1)\sin^2\theta\right] \\ + A\left[\sin(\theta-\alpha) - \lambda_{xz}\cos\theta\,\cos\alpha\right]^2, \end{aligned} \tag{4}$$

from which in the limit of small rotation angles and shears relative to the undistorted state, microscopic expressions can be derived for the de Gennes coefficients, *viz.*, $D_1 = \mu(\ell_\parallel - \ell_\perp)^2/(\ell_\parallel\ell_\perp)$, $D_2 = \mu(\ell_\parallel^2 - \ell_\perp^2)/(\ell_\parallel\ell_\perp)$. The relation between continuum elastic and microscopic theories of elastomers has been examined by Olmsted [22].

2.2 The evolution equations

The simplest dynamical (*i.e.*, non-equilibrium) model is constructed by equating the rate of change of the relevant variables to the gradient of the FED, corresponding to two non-conserved order parameters:

$$\frac{\partial\theta}{\partial t} = -\Gamma_\theta\frac{\partial(2f/\mu)}{\partial\theta}, \tag{5}$$

$$\frac{\partial\lambda_{xz}}{\partial t} = -\Gamma_\lambda\frac{\partial(2f/\mu)}{\partial\lambda_{xz}}, \tag{6}$$

where Γ_θ, Γ_λ are, respectively, the director and strain 'mobilities': $\Gamma_\theta = \mu/(2\gamma_1)$, with γ_1 the LC viscosity. The model thus constructed is purely dissipative, *i.e.*, it does not include any coupling to hydrodynamic variables (only sound waves, as the elastomer is a solid). This may appear a drastic simplification, but notice that the speed of sound in an elastomer is of the order of m/s. As a typical experimental sample is a few centimeters in size, any sound waves will traverse it in $\sim 10^{-2}$ s, much less than the duration of a reorientation experiment ($\sim 10^2$ s, see [17]). Moreover, we are neglecting solvent diffusion and related effects.

3 Results

3.1 Asymptotic analysis

Equations (5, 6) are non-linear ordinary differential equations, and can only be solved numerically. However, it is instructive to study their asymptotic behaviour, when $\theta \sim \alpha$ and $\lambda_{xz} \sim 0$. This is amenable to analytic treatment in the case where the strain λ_{xz} relaxes much faster than the director (*i.e.*, $\Gamma_\lambda/\Gamma_\theta \gg 1$), corresponding to the network 'instantaneously' adopting such configuration as minimises f^* at the given $\theta = \theta(t)$. Minimisation of f^* with respect to λ_{xz} yields, for $\alpha = 0$,

$$\lambda_{xz}^* = \frac{(Ar - r + 1)\,\sin 2\theta}{Ar + r + 1 + (Ar - r + 1)\,\cos 2\theta}\,. \tag{7}$$

Inserting equation (7) into the FED, equation (4), and expanding to $\mathcal{O}(\theta^4)$, we obtain

$$\frac{1}{\mu}f^*_{\rm asymp}(\theta) = \frac{3}{2} - \frac{1}{2}p\,\theta^2 + \frac{1}{4}q\,\theta^4 + \mathcal{O}(\theta^6), \tag{8}$$

$$p = -\frac{A\,(r-2)^2}{1+Ar} \le 0, \tag{9}$$

$$q = \frac{2\left(3 - 4A - 6r - 2Ar - 4A^2r + 3r^2 + 5Ar^2 + 7A^2r^2 - A^2r^3\right)}{3\,(1+Ar)^2}\,. \tag{10}$$

If $A = 0$, $p = 0$ and $q = 2(r-1)^2$, *i.e.*, the harmonic term vanishes and quartic (soft) elasticity dominates; this has important qualitative consequences, as we shall see shortly. Equation (5) with equation (8), *viz.*

$$\frac{\partial\theta}{\partial t} = -2\Gamma_\theta\left(-p\,\theta + q\,\theta^3\right), \tag{11}$$

is readily integrated to give (recall that $p \le 0$)

$$\theta(t) = \left(-\frac{p}{q}\right)^{1/2}\left[\left(1 - \frac{p}{q\,\theta_0^2}\right)\exp\left(-4p\Gamma_\theta t\right) - 1\right]^{-1/2}, \tag{12}$$

where $\theta_0 \equiv \theta(t=0)$. In the soft elastic limit, $A \to 0$, equation (12) becomes

$$\theta(t) = \left[8(r-1)^2\Gamma_\theta t + \theta_0^{-2}\right]^{-1/2}. \tag{13}$$

At very long times ($t \gg \Gamma_\theta^{-1}$) we have, from equations (13, 12), respectively,

$$\theta(t) \sim t^{-1/2} \qquad (A = 0), \tag{14}$$

$$\theta(t) \sim \exp\left(2p\Gamma_\theta t\right) \qquad (A \neq 0), \tag{15}$$

as can be inferred by inspection of equation (11). Thus a *semi-soft* medium relaxes exponentially, while a *soft* medium exhibits algebraic (power-law) relaxation. (Indeed, one intuitively expects a rigid medium to relax faster than a soft one.) The qualitatively different behaviours are related to the presence ($A \neq 0$) or absence

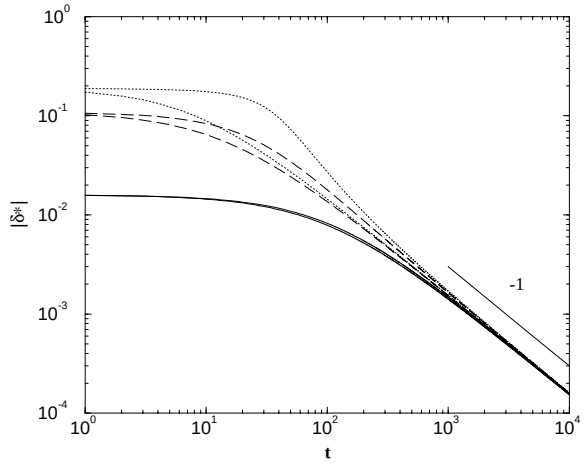

Fig. 2. Reduced optical path difference δ^* *vs.* time in a soft elastomer ($A = 0$) with fast strain ($\Gamma_\theta/\Gamma_\lambda = 0.1$) and no pretilt ($\alpha = 0$). The upper line of each style is the numerical result, the lower one the analytical approximation (see the text for details). $\theta_0 = 15°$ (solid lines), 45° (dashed), and 75° (dotted). The short straight line on the right gives the predicted asymptotic slope, -1. This is a double logarithmic plot.

($A = 0$) of a quadratic term in $f^*_{\rm asymp}$, equations (8, 9), which modifies the torque on the director: soft elasticity is 'critical' or 'massless', whereas semi-soft elasticity is 'non-critical' or 'massive'; by analogy one might say that soft elastic modes are 'critically slowed down' [23]. Although this result was obtained in the fast-strain limit, it appears to be true for all ratios $\Gamma_\theta/\Gamma_\lambda$ investigated, see Figure 4, with the same power-law exponent.

If $\alpha \neq 0$ it is convenient to rewrite the FED in terms of $\omega = \theta - \alpha$. In the same fast strain limit as above, we now get

$$\frac{1}{\mu} f^*_{\rm asymp}(\omega) = \frac{3}{2} - \frac{1}{2} p'\,\omega^2 + \frac{1}{3}\kappa\,\omega^3 + \frac{1}{4} q'\,\omega^4 + \mathcal{O}(\omega^5). \tag{16}$$

Here p', κ, and q' are given by rather long (and not particularly useful in the present context) expressions. The most important change is that for non-zero pretilt, there is always a non-vanishing p' (*i.e.*, conventional harmonic elasticity), and therefore exponential decay, *even if* $A = 0$. Physically, this means that *no soft deformations are possible in the present geometry starting from a director at an angle* $\alpha \neq 0$ *to the bounding plates* (with the obvious exception of trivial body rotations). Such a conclusion follows from the analysis of Olmsted [22]: the form of our strain tensor, equation (1), as dictated by the requirements that the plates be fixed and that all λ_{ij} be functions of z only, is incompatible with the general form of a soft deformation, equation (3.6) in [22], which would contain more non-vanishing components. Because an identically null pretilt is difficult to achieve in practice, we are led to expect that virtually all elastomers will behave (dynamically at least) as semi-soft, *i.e.*, will relax exponentially [24]. In addition, equation (16) contains a cubic term, which implies that a closed expression for $\theta(t)$ analogous to equation (13) can no longer be derived.

Experimentally, one measures by conoscopy the intensity of light transmitted through the cell. This is a function of the difference in optical path for ordinarily and extraordinarily polarised rays, $\delta = d(n_{\rm e} - n_{\rm o})/\lambda$, where d is the cell thickness, λ is the wavelength of light, and $n_{\rm e} - n_{\rm o}$ the birefringence, with $n_{\rm e}$ and $n_{\rm o}$ the extraordinary and ordinary refractive indices, respectively. For normal light incidence, the birefringence will change as the director rotates:

$$\delta = \frac{d}{\lambda}\left[n_{\rm eff}(\alpha) - n_{\rm eff}(\theta)\right], \tag{17}$$

$$n^2_{\rm eff}(\Theta) = \frac{n^2_{\rm e}\, n^2_{\rm o}}{n^2_{\rm o} + (n^2_{\rm e} - n^2_{\rm o})\sin^2\Theta}, \tag{18}$$

where the dummy argument $\Theta = \alpha$ or θ. In the small θ limit, equation (18) gives

$$n_{\rm eff}(0) - n_{\rm eff}(\theta) = \frac{n_{\rm e}}{2n_0^2}\left(n^2_{\rm e} - n^2_{\rm o}\right)\theta^2 - \frac{n_{\rm e}}{4n_0^2}\left[\frac{3}{2n_0^2}\left(n^2_{\rm e} - n^2_{\rm o}\right)^2 + \frac{2}{3}\left(n^2_{\rm e} - n^2_{\rm o}\right)\right]\theta^4 + \mathcal{O}(\theta^6), \tag{19}$$

whence it follows that, in the asymptotic regime ($t \to \infty$),

$$\delta \sim t^{-1} \qquad (A = 0), \tag{20}$$

$$\delta \sim \exp\left(4p\Gamma_\theta t\right) \qquad (A \neq 0). \tag{21}$$

3.2 Numerical solution

Equations (5, 6) have been integrated using NAG routine D02BDF, for $r = 1.44$ (appropriate to acrylates [11]), $n_{\rm e} = 1.74$, $n_{\rm o} = 1.54$ [17], and $\theta_0 = 15°, 30°, 45°, 60°, 75°$. Each starting angle is the initial orientation imposed by a field of varying strength along the z-axis: the stronger the field, the closer θ_0 is to 90°, as can be seen by minimising the FED for $E \neq 0$. $\lambda_{xz,0} \equiv \lambda_{xz}(t = 0)$ is chosen to be λ^*_{xz} evaluated at $\theta = \theta_0$; this corresponds to an initially-relaxed strain. As a check on the consistency of the theory, Figures 2 and 3 compare the numerically calculated reduced optical path difference, $\delta^* = \lambda\delta/d$ (Eqs. (17, 18) with Eq. (5)) with its asymptotic behaviour for $\Gamma_\theta/\Gamma_\lambda = 0.1$ (Eqs. (17, 18) with Eqs. (12) or (13)). Here, and in the remainder of this paper, time is measured in units of Γ_λ^{-1}.

The slowing-down effect of soft elasticity ($A = 0$) is illustrated in Figure 4 for $\theta_0 = 30°$ and $\alpha = 0$ (no pretilt). This is the more marked the faster the director relative to strain. On the other hand, the starting value of θ substantially affects the short-time (pre-asymptotic) behaviour, especially in the case of fast strain (see Fig. 5), but has no influence on the long-time evolution, which depends only on the shape of the free energy landscape near its minima. In this connection it is also noteworthy that $\lambda_{xz}(t)$ (shown

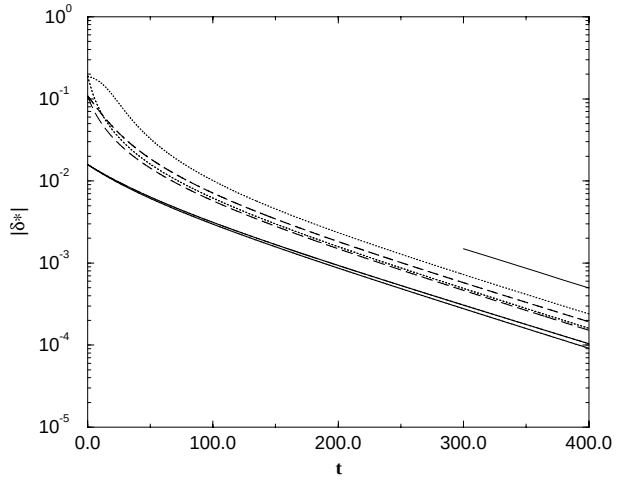

Fig. 3. Same as Figure 2 but for semi-soft elasticity ($A = 0.1$). The short straight line on the right gives the predicted asymptotic slope, -0.010965 (see Eq. (21)). Note this is now a linear-logarithmic plot.

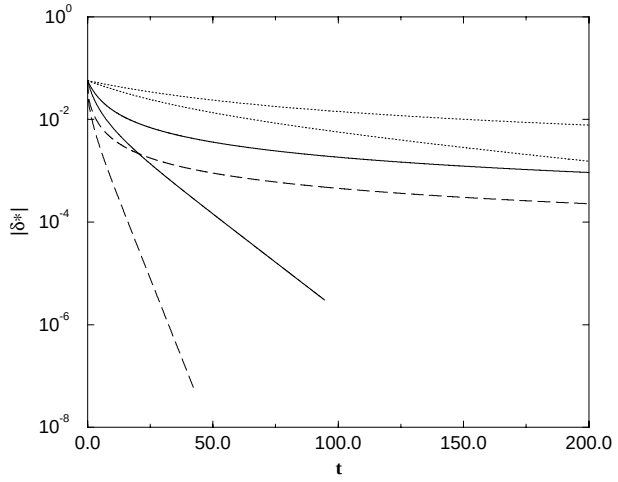

Fig. 4. Effect of semi-softness: reduced optical path difference δ^* *vs.* time for $\theta_0 = 30^\circ$ and $\alpha = 0$. The upper line of each style is the soft elasticity result ($A = 0$), the lower one the semi-soft case ($A = 0.1$). Solid lines: $\Gamma_\theta/\Gamma_\lambda = 1$; dashed lines: $\Gamma_\theta/\Gamma_\lambda = 10$; dotted lines: $\Gamma_\theta/\Gamma_\lambda = 0.1$. The effect of semi-softness is particularly pronounced when the director is the faster variable.

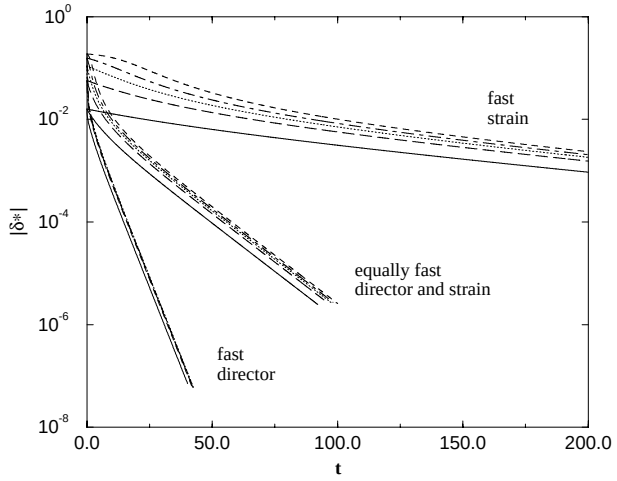

Fig. 5. Effect of different starting angles: reduced optical path difference δ^* *vs.* time for a semi-soft elastomer ($A = 0.1$) with zero pretilt ($\alpha = 0$) and $\Gamma_\theta/\Gamma_\lambda = 10$ (fast director, lower set of curves), $\Gamma_\theta/\Gamma_\lambda = 1$ (equally fast director and strain, middle set of curves), and $\Gamma_\theta/\Gamma_\lambda = 0.1$ (fast strain, upper set of curves). Solid lines: $\theta_0 = 15^\circ$; dashed lines: $\theta_0 = 30^\circ$; dotted lines: $\theta_0 = 45^\circ$; dash-dotted lines: $\theta_0 = 60^\circ$; short-dashed lines: $\theta_0 = 75^\circ$.

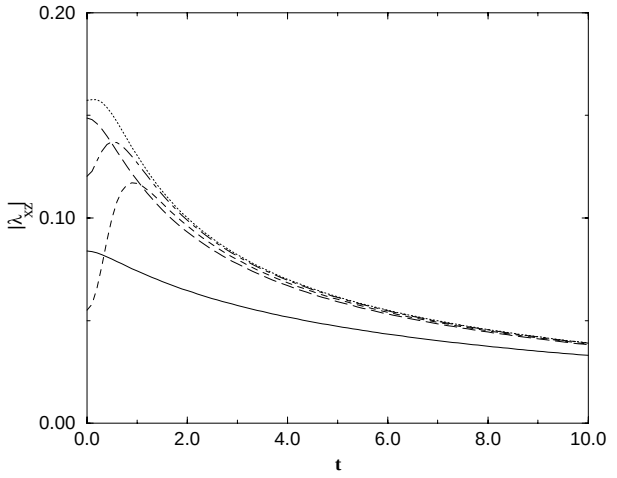

Fig. 6. Modulus of strain λ_{xz} *vs.* time for a soft elastomer ($A = 0$) with pretilt $\alpha = 3^\circ$ and fast director ($\Gamma_\theta/\Gamma_\lambda = 10$). Solid line: $\theta_0 = 15^\circ$; dashed line: $\theta_0 = 30^\circ$; dotted line: $\theta_0 = 45^\circ$; dash-dotted line: $\theta_0 = 60^\circ$; short-dashed line: $\theta_0 = 75^\circ$. Results are qualitatively the same for all combinations of A, α and $\Gamma_\theta/\Gamma_\lambda$.

in Fig. 6) is non-monotonic for $\theta_0 \geq 45^\circ$, owing to the minimum in $\lambda^*_{xz}(\theta)$ at $\theta \sim 40^\circ$. By contrast, inclusion of a non-zero pretilt has more subtle consequences: it speeds up soft elastomers (Fig. 7), but can slow down semi-soft ones (Fig. 8). So far I have been unable to account for this analytically (see remark following Eq. (16) above): intuitively one would expect $\alpha \neq 0$ always to speed up the dynamics for a given θ_0, as it corresponds to reorientation through a smaller angle. The pretilt seems strongly correlated with the mobility: whereas the splitting of the curves for $\Gamma_\theta/\Gamma_\lambda = 10$ in Figures 7 and 8 is substantial, that for $\Gamma_\theta/\Gamma_\lambda = 0.1$ is barely noticeable.

4 Discussion

Do these results shed any light on Meyer's *et al.*'s findings? Start by noting that a real-life elastomer if very likely

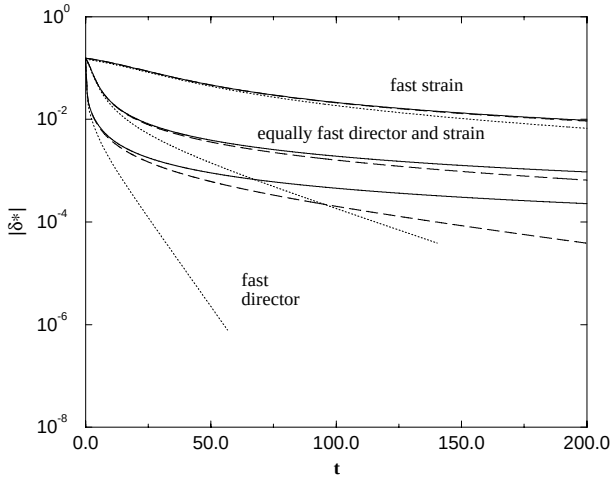

Fig. 7. Effect of pretilt: reduced optical path difference δ^* *vs.* time for a soft elastomer ($A = 0$) initially at $\theta_0 = 60°$, and $\Gamma_\theta/\Gamma_\lambda = 10$ (fast director, lower set of curves), $\Gamma_\theta/\Gamma_\lambda = 1$ (equally fast director and strain, middle set of curves), and $\Gamma_\theta/\Gamma_\lambda = 0.1$ (fast strain, upper set of curves). Solid lines: $\alpha = 0°$; dashed lines: $\alpha = 3°$; dotted lines: $\alpha = 10°$. In all cases, increasing the pretilt accelerates the dynamics.

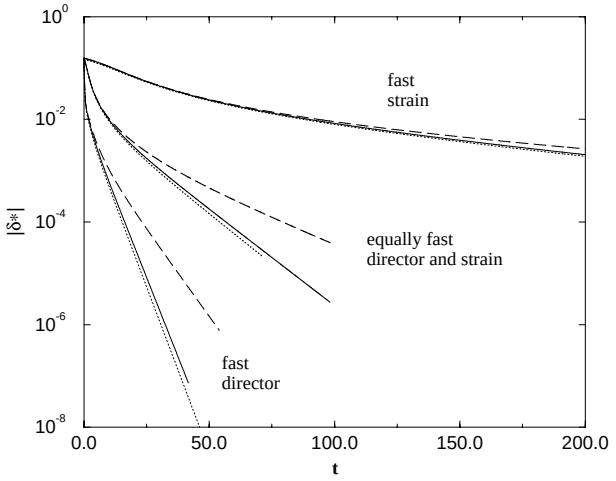

Fig. 8. Same as Figure 7, but for the semi-soft case ($A = 0.1$). Unlike in the soft elastomer, increasing the pretilt first decelerates ($\alpha = 3°$) the decay, although at larger pretilts ($\alpha = 10°$) the previously observed accelerative trend is recovered.

semi-soft, or 'non-critical' (see discussion after Eq. (3)). Then the theory predicts purely exponential long-time behaviour. Yet this does not set in until a time $t_{\rm asymp}$ which is a function of A, of the starting angle θ_0, the pretilt α, and the relative mobilities of director and strain, $\Gamma_\theta/\Gamma_\lambda$. As in Figure 8 it is the fast-strain curves that cross the latest into the exponential regime, we can, using equation (21) and $\mu \sim 10^3 - 10^4$ J/m^3 [19], $\gamma_1 = 2.2\times10^4$ P [17], derive upper bounds for $t_{\rm asymp} \sim 100/\Gamma_\lambda = 1000/\Gamma_\theta \sim 4$ s and for the exponential relaxation time $\tau \sim (-4p'\Gamma_\theta)^{-1} \sim 0.4/A - 4/A$ s. Hence $\tau \sim 50$ s as in [17] is achievable if $A \sim 8\times10^{-2} - 8\times10^{-3}$, and the theory is also compatible with a decay that is experimentally indistinguishable from exponential (the possible non-exponential character originally reported by Meyer *et al.* is now attributed to difficulty in preparing a sufficiently homogeneous thin sample [19]). Furthermore, as remarked in Section 2, A can be independently measured from, *e.g.*, the strain threshold for director rotation in an elastomer stretched perpendicular to the initial nematic alignment [15].

From Figure 3 of [17] one estimates the accuracy of Meyer *et al.*'s measurements as $\sim 10^{-2}$, which means that the asymptotic regimes of Figures 4–8 are practically inaccessible. The best prospect of experimental verification thus seems to be to look at the early-time shape of the δ^* curves for large starting angle θ_0, see Figure 5. Alternatively one could follow the evolution of strain, see Figure 6, by observing, along the z-axis, the motion of 'tracer' particles (*e.g.*, impurities in the LC gel) in a direction in the plane of the cell; such displacements as have been seen so far are consistent with the picture proposed here and in [19].

I have constructed perhaps the simplest model for the dynamics of reorientation of a confined nematic elastomer initially (mis)aligned by an external field. Within this framework it is possible to interpret the dynamical observations of Meyer and co-workers. Although experimental validation for this one particular system may present some problems, predictions have been made for the behaviour of elastomers characterised by a whole range of material parameters and different initial and final alignments, so adequate tests should be feasible.

I thank M. Warner and E.M. Terentjev for many stimulating discussions and advice, and for a critical reading of the manuscript; R.B. Meyer for correspondence; and P.D. Olmsted for clarification of some important points concerning soft elasticity. The financial support of the EPSRC (United Kingdom) is gratefully acknowledged.

References

1. P.G. de Gennes, Phys. Lett. A **28**, 725 (1969).
2. P.G. de Gennes, C. R. Acad. Sci. B **281**, 101 (1975).
3. G.G. Barclay, C.K. Ober, Prog. Polym. Sci. **18**, 899 (1993).
4. M. Warner, E.M. Terentjev, Prog. Polym. Sci. **21**, 853 (1996).
5. J. Schätzle, W. Kaufhold, H. Finkelmann, Makromol. Chem. **190**, 3269 (1989).
6. G.R. Mitchell, M. Coulter, F.J. Davis, W. Guo, J. Phys. II France **2**, 1121 (1992).
7. C.H. Legge, F.J. Davis, G.R. Mitchell, J. Phys. II France **1**, 1253 (1991).
8. F.J. Davis, G.R. Mitchell, Polym. Commun. **28**, 8 (1987).

9. P. Bladon, E.M. Terentjev, M. Warner, Phys. Rev. E **47**, R3838 (1993).
10. P. Bladon, E.M. Terentjev, M. Warner, J. Phys. II France **4**, 75 (1994).
11. G.R. Mitchell, F.J. Davis, W. Guo, Phys. Rev. Lett. **71**, 2947 (1993).
12. P.M.S. Roberts, G.R. Mitchell, F.J. Davis, J. Phys. II France **7**, 1337 (1997).
13. I. Kundler, H. Finkelmann, Makromol. Chem. Rapid Commun. **16**, 679 (1995).
14. G.C. Verwey, M. Warner, H. Terentjev, J. Phys. II France **6**, 1273 (1996).
15. H. Finkelmann, I. Kundler, E.M. Terentjev, M. Warner, J. Phys. II France **7**, 1059 (1997).
16. M. Warner, Phil. Trans. R. Soc. Lond. A **348**, 59 (1994).
17. C.-C. Chang, L.-C. Chien, R.B. Meyer, Phys. Rev. E **56**, 595 (1997).
18. P.G. de Gennes, in *Liquid Crystals of One- and Two-dimensional Order*, edited by W. Helfrich, G. Heppke (Springer, Berlin, 1980).
19. E.M. Terentjev, M. Warner, R.B. Meyer, J. Yamamoto, submitted to Phys. Rev. E.
20. See, *e.g.*, C.G. Gray, K.E. Gubbins, *Theory of Molecular Fluids* (Clarendon Press, Oxford, 1984), Vol. 1, Appendix A.
21. For a Frank elastic constant $K = 8 \times 10^{-12}$ N, a layer thickness $d = 124$ μm [17], and a rubber modulus $\mu = 1.6 \times 10^2$ J/m^3 [19], $\mu d^2/K \sim 3 \times 10^5 \gg 1$.
22. P.D. Olmsted, J. Phys. II France **4**, 2215 (1994).
23. See, *e.g.*, P.M. Chaikin, T.C. Lubensky, *Principles of Condensed Matter Physics* (Cambridge University Press, Cambridge, 1995).
24. As can be inferred from solving the linearised versions of equations (5, 6).